

Sulforhodamine B Intercalated Layered Double Hydroxide Thin Film with Polarized Photoluminescence

Dongpeng Yan, Jun Lu, Min Wei, David G. Evans, and Xue Duan

J. Phys. Chem. B, **2009**, 113 (5), 1381-1388 • DOI: 10.1021/jp8084217 • Publication Date (Web): 14 January 2009

Downloaded from <http://pubs.acs.org> on February 18, 2009

More About This Article

Additional resources and features associated with this article are available within the HTML version:

- Supporting Information
- Access to high resolution figures
- Links to articles and content related to this article
- Copyright permission to reproduce figures and/or text from this article

[View the Full Text HTML](#)

Sulforhodamine B Intercalated Layered Double Hydroxide Thin Film with Polarized Photoluminescence

Dongpeng Yan, Jun Lu,* Min Wei,* David G. Evans, and Xue Duan

State Key Laboratory of Chemical Resource Engineering, Beijing University of Chemical Technology, Beijing, 100029, P. R. China

Received: September 22, 2008; Revised Manuscript Received: November 28, 2008

Sulforhodamine B (SRB) and dodecylbenzenesulfonate (DBS) with different molar ratios cointercalated into the interlayer region of Mg–Al-layered double hydroxide (SRB-DBS/LDH) were prepared. The structure and chemical composition of the composites were characterized by X-ray diffraction, elemental analysis, thermogravimetry, and differential thermal analysis (TG-DTA). Fluorescence spectra demonstrate that the sample with 4.76% SRB molar percentage, with respect to the total organic material, exhibits the optimal luminous intensity. The fluorescence lifetime of SRB in SRB-DBS/LDH is enhanced significantly compared with that of pristine SRB in solution (4.14 vs 2.05 ns). SRB-DBS/LDH thin films on the quartz substrates were constructed by the solvent evaporation method. Steady-state polarization photoemission spectra show that the luminescence anisotropy of SRB-DBS/LDH thin films ($r = 0.10$) was enhanced remarkably compared with that of a powder sample ($r = 0 \pm 0.01$) at ambient temperature, whereas the anisotropy of both film and powder samples was largely improved at low temperature (77 K). Furthermore, the SRB-DBS/LDH thin films exhibit a luminescence anisotropy decay effect in the range of their fluorescence lifetime. These results demonstrate that the SRB-DBS/LDH thin films could be used as a good candidate for the immobilization of laser dyes and polarized luminescence materials.

1. Introduction

The hybrid materials with guest dye doping into host matrixes are considered as good candidates for solid-state tunable dye laser application.¹ The advantages of these materials with respect to dye solution can be mainly due to the following reasons: first, the solid matrixes can offer a confined and stable environment for the immobilization of dye molecules, which is a prerequisite and important characteristic of a solid-state dye laser. Second, the homogeneous distribution of the dye molecules in solid matrixes at the molecular level based on host–guest interactions (e.g., the electrostatic, Van der Waals interaction, or even covalent bonding) can avoid dye aggregation and fluorescence quenching effectively. Last but not least, the solid matrixes enhance the optical and thermal stability of the dye molecules and reduce the environmental pollution and operational risk, which meets the fabrication needs of solid-state light-emission devices.

One important family of such solid host matrixes are layered double hydroxides (LDHs), also known as “anion clay” compounds, which can be described by the general formula $[M^{II}_{1-x}M^{III}_x(OH)_2]^{z+}A^{n-}_{z/n} \cdot yH_2O$. M^{II} and M^{III} are divalent and trivalent metals respectively; A^{n-} is the anion to compensate for the positive charge of the hydroxide layers. Recently, LDHs have received much attention due to the potential applications in the fields of catalysis,² separation process,³ biology, and medicine.⁴ Various dye molecules, such as methyl orange,⁵ fluorescein,⁶ perylene chromophores,⁷ naphthalene,⁸ and pyrene derivatives⁹ were intercalated into the LDHs for the requirement of enhancing the luminous efficiency of dye. The intercalated dye molecules may exhibit some additional photophysical

behavior in a two-dimensional (2D) confined environment that is absent in solution. Moreover, the host–guest interaction offers a higher mechanical, thermal, and chemical stability for the dye molecules. Generally, low-dimensional (1D or 2D), asymmetric, and ordered luminescent structure exhibits polarized photoemission properties, such as nanorods,¹⁰ nanotubes,¹¹ and core–shell nanoparticles.¹² Furthermore, oriented self-emissive structures in a host matrix¹³ also present well-polarized light-emission character. The ordered assembly of dye molecules into the layered structure is undoubtedly favorable to produce a uniform orientation of transition dipole moment for polarized photoemission. Since LDH with 2D layered structure is intrinsically anisotropic, the dye molecule with single transition dipole moment preferentially oriented between LDH interlayer may exhibit special anisotropic photoemission characteristics. Recently, the thin film preparation of LDHs has become a promising subject for the functional application of LDHs-based materials.¹⁴ Compared with the dye-intercalated LDH powder with the house-of-card structures,¹⁵ its thin films exhibit prominent preferred orientation and polarized photoemission, providing potential applications in the field of polarized light-emitting devices.¹⁶

The fluorescence dye aggregates, however, can still be found in some dye-intercalated layered matrix systems. Gago found that dye dimers exit together with monomers in 1-pyrene-sulfonate (PS) intercalated Zn–Al-LDH.⁹ Bauer et al.⁷ reported that the composites of perylene bisimidetetrasulfonate (PBITS) intercalated Zn–Al-LDH show complete fluorescence quenching, and some cointercalated nitrates and hydroxyl ions can not suppress the formation of dye aggregates. Therefore, the key problem is how to effectively avoid the formation of dye aggregates in the gallery of LDH.

Rhodamine dyes are one of the most important laser dyes, and aggregation of rhodamine dyes is well-documented in the

* To whom correspondence should be addressed. E-mail: lujun@mail.buct.edu.cn (J.L.), weimin@mail.buct.edu.cn (M.W.); fax: +86-10-64425385; phone: +86-10-64412131.

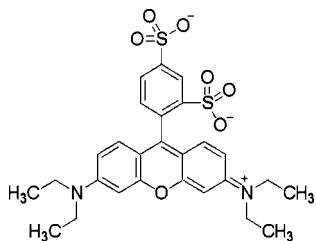


Figure 1. The structure of sulforhodamine B (SRB).

literature. The studies on the incorporation of rhodamine and cation clays (both adsorption and intercalation) have been carried out during the past few years;^{17a-f} to the best of our knowledge, however, no photoemission property of rhodamine intercalated anion clays has been reported. In the present work, sulforhodamine B (SRB) (shown in Figure 1) and dodecylbenzene-sulfonate (DBS) were chosen to be the dye molecule and the cointercalated agent, respectively. The employment of DBS is to provide the SRB molecule with a homogeneous nonpolar environment so as to prevent its aggregation and thus enhance the photoemission properties. The correlation between SRB luminescence and its concentration was explored, and the optimal luminescence intensity was obtained. Furthermore, the SRB-DBS/LDH thin films were prepared by the solvent evaporation method, and the orientation behavior of dye in the gallery of LDH was further investigated by time-resolved photoemission anisotropy measurement. This work demonstrates that the cointercalation method is a favorable approach to prevent dye aggregation and to enhance its luminescence efficiency, and it also provides a detailed understanding of the polarization photoemission characteristics for dye-intercalated LDH. It can be expected that SRB intercalated LDH films may have potential application in the field of polarized luminescence materials.

2. Experimental Section

2.1. Materials. NaOH (AR), Mg(NO₃)₂·6H₂O (AR), and Al(NO₃)₃·9H₂O (AR) were purchased from Beijing Chemical Plant Limited and were used without further purification. Sodium sulforhodamine B (SRB, also named Acid Red 52) and sodium dodecylbenzenesulfonate (DBS, >95%) were purchased from Sigma Chemical. Co. Ltd.

2.2. Precursor Solutions. Solution A: Mg·(NO₃)₂·6H₂O (0.05 mol), Al(NO₃)₃·9H₂O (0.025 mol), DBS (*a* mol) and SRB (*b* mol, in which *a* + *b* = 0.025 mol; *a*:*b* = 100:1; 100:2; 100:5; 100:8; 100:10; 100:20; 3:1; 1:1; 1:3; 0. *x* % = *a*/(*a*+*b*)) dissolved in 70 mL of deionized water and 35 mL of anhydrous ethanol. Solution B: NaOH (0.15 mol) dissolved in 105 mL of deionized water.

2.3. Synthesis of DBS-SRB/LDH Powder. Solution A (105 mL) and solution B (105 mL) were simultaneously added to a colloid mill, rotating at 3000 rpm, and mixed for 1 min. The resulting slurry was removed from the colloid mill and was sealed into 90 mL Teflon-lined stainless steel autoclaves, purged with nitrogen atmosphere for 5 min, and heated at 100 °C for 1 day. The products were washed with hot, distilled water and anhydrous ethanol for several times until the cleaning liquid was colorless and then dried in a vacuum at 60 °C for 6 h.

2.4. Synthesis of DBS-SRB/LDH Thin Film. The film of DBS-SRB/LDH was prepared by the solvent evaporation method; a suspension of SRB-DBS/LDH in ethanol (1 mg/mL) was thoroughly dispersed under ultrasonic and then extended on a quartz substrate that was fully cleaned by an ultrasonic anhydrous ethanol bath.

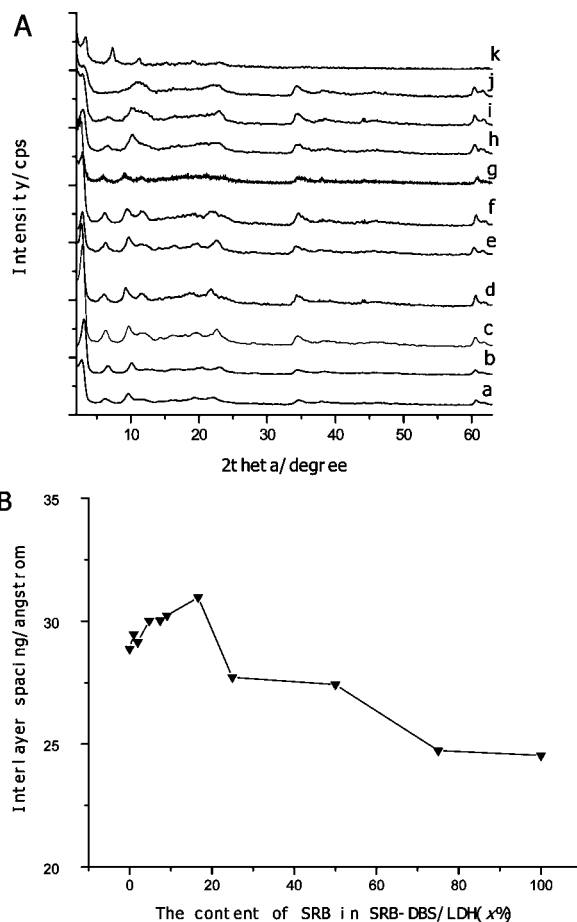


Figure 2. (A) Powder XRD patterns of SRB-DBS/LDH (*x*%). (a, 0%; b, 0.99%; c, 1.96%; d, 4.76%; e, 7.41%; f, 9.09%; g, 16.67%; h, 25.0%; i, 50.0%; j, 75.0%; k, 100%). (B) The plot of interlayer spacings vs SRB concentration.

2.5. Characterization. Powder XRD patterns of the samples were recorded using a Rigaku XRD-6000 diffractometer under the following conditions: 40 kV, 30 mA, Cu K α radiation. The powder samples were step-scanned in step of 0.04° (2θ) in the range from 2 to 70° using a count time of 10 s/step. The morphology of SRB-DBS/LDH thin film was investigated using a scanning electron microscope (SEM Hitachi S-3500) equipped with an EDX attachment (EDX Oxford Instrument Isis 300), and the accelerating voltage applied was 20 kV. The surface roughness data were obtained using the atomic force microscopy (AFM) software (Digital Instruments, Version 6.12). Thermogravimetry and differential thermal analysis (TG-DTA) were carried out on a PCT-1A thermal analysis system under ambient atmosphere with a heating rate of 10 °C/min. Elemental analyses were performed by ICP atomic emission spectroscopy using solutions prepared by dissolving the samples in dilute HNO₃. Carbon, hydrogen, and nitrogen analyses were carried out using a Perkin-Elmer Elementarvario elemental analysis instrument. The solid fluorescence spectra of powders were performed on a RF-5301PC fluorospectrophotometer under the identical condition with excitation wavelength of 360 nm and emission spectra in the range 550–700 nm. The width of both the excitation and emission slit is 3 nm. Steady-state and time-decay polarized photoluminescence measurements were recorded with an Edinburgh Instruments' FLS 920 fluorimeter. The emission spectra and lifetime were measured by exciting the samples at 570 nm with a 450 W Xe lamp and nanosecond flashlamp, respectively. Also, the percentage contribution of each

TABLE 1: Chemical Compositions of SRB-DBS/LDH (x%) with Different SRB Content

sample initial x (%)	chemical composition	Mg/Al ratio	sample final x (%)
0	Mg _{0.731} Al _{0.269} (OH) ₂ (C ₁₈ H ₂₉ SO ₃) _{0.187} (OH) _{0.082} · 0.58H ₂ O	2.72	0
9.09	Mg _{0.691} Al _{0.309} (OH) ₂ (C ₁₈ H ₂₉ SO ₃) _{0.289} (C ₂₇ H ₂₉ N ₂ O ₇ S ₂) _{0.020} · 0.24H ₂ O	2.24	6.47
16.67	Mg _{0.736} Al _{0.264} (OH) ₂ (C ₁₈ H ₂₉ SO ₃) _{0.228} (C ₂₇ H ₂₉ N ₂ O ₇ S ₂) _{0.036} · 0.86H ₂ O	2.79	13.64
25.0	Mg _{0.745} Al _{0.255} (OH) ₂ (C ₁₈ H ₂₉ SO ₃) _{0.215} (C ₂₇ H ₂₉ N ₂ O ₇ S ₂) _{0.040} · 0.93H ₂ O	2.92	15.69
50.0	Mg _{0.744} Al _{0.256} (OH) ₂ (C ₁₈ H ₂₉ SO ₃) _{0.122} (C ₂₇ H ₂₉ N ₂ O ₇ S ₂) _{0.134} · 1.17H ₂ O	2.91	52.34
75.0	Mg _{0.759} Al _{0.241} (OH) ₂ (C ₁₈ H ₂₉ SO ₃) _{0.035} (C ₂₇ H ₂₉ N ₂ O ₇ S ₂) _{0.206} · 1.32H ₂ O	3.15	85.48
100.0	Mg _{0.719} Al _{0.281} (OH) ₂ (C ₂₇ H ₂₉ N ₂ O ₇ S ₂) _{0.281} · 0.49H ₂ O	2.56	100.0

lifetime component to the total decay was calculated with the F900 Edinburgh instruments software. The solid UV-vis adsorption spectra were recorded in reflectance mode using an integration sphere in the range from 210 to 800 nm on a Shimadzu U-3000 spectrophotometer. The width of the slit is 1.0 nm, and BaSO₄ was used as reference.

3. Results and Discussion

In this work, the method of separate nucleation and aging steps (SNAS)¹⁸ was used to prepare SRB and DBS cointercalated Mg-Al-LDH in order to obtain uniform size distribution

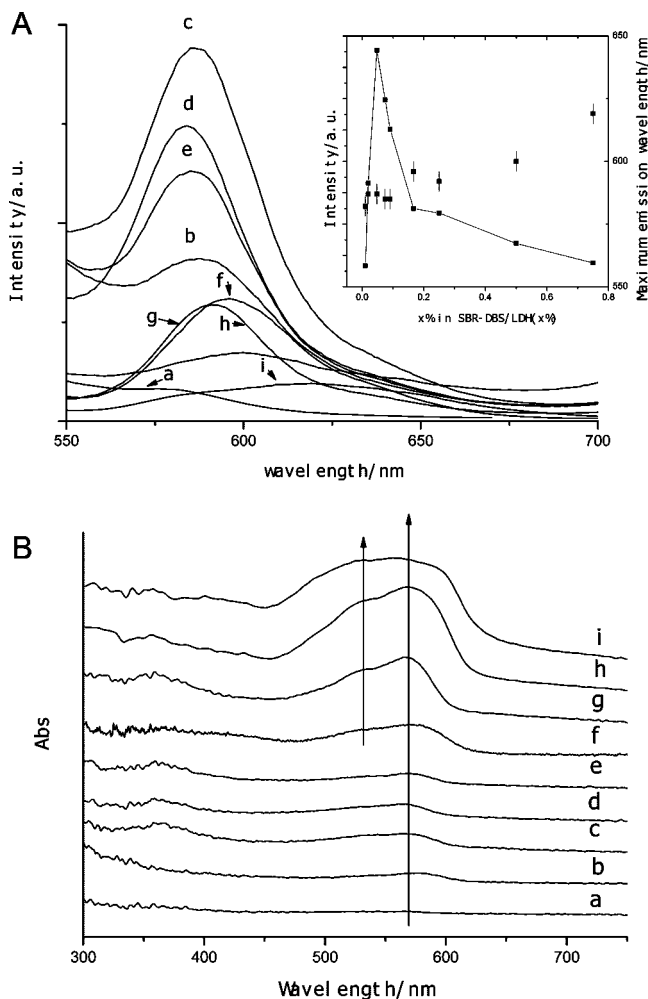


Figure 3. (A) The photoemission spectra of SRB-DBS/LDH with the excitation wavelength of 360 nm. The inset plot shows the fluorescence intensity and the maximum emission wavelength varying with the increase of SRB content in the SRB-DBS/LDH(x %): (a) 0.99%, (b) 1.96%, (c) 4.76%, (d) 7.41%, (e) 9.09%, (f) 16.67%, (g) 25.0%, (h) 50.0%, (i) 75.0%. (B) The solid UV-vis absorption spectra of SRB-DBS/LDH (x%). (a, 0.99%; b, 1.96%; c, 4.76%; d, 7.41%; e, 9.09%; f, 16.67%; g, 25.0%; h, 50.0%; i, 75.0%).

TABLE 2: Fluorescence Decay Data of the Powder Samples of SRB-DBS/LDH (x%)^a

x (%)	n	τ_i (ns)	A_i (%)	$\langle\tau\rangle$ (ns)	χ^2
0.99	1	3.304	100.00	3.308	1.712
	2	1.806	31.40		1.167
4.76	1	3.996	68.60	4.034	1.355
		3.710	100.00		1.185
	2	8.606	12.08		1.185
9.09	1	3.406	87.92	4.142	1.417
		4.106	100.00		1.254
	2	3.302	47.18		1.254
	4.892	52.82	1.254		
16.67	1	3.781	100.00	3.757	1.495
		1.261	8.22		1.142
	2	3.981	91.78		1.142
25.0	1	1.284	100.00	1.625	1.195
		1.340	94.35		1.168
	2	6.390	5.65		1.168

^a n is the mono- or double-exponential fitting of the fluorescence decay curve; τ_i is the fluorescence lifetime. For $n = 1$, the lifetime is τ_1 , and for $n = 2$, τ_1 and τ_2 correspond to two lifetimes; A_i is the percentage of τ_i . The goodness of fit is indicated by the value of χ^2 . In the double-exponential case, $\langle\tau\rangle = A_1\tau_1 + A_2\tau_2$; $A_1 + A_2 = 1$.

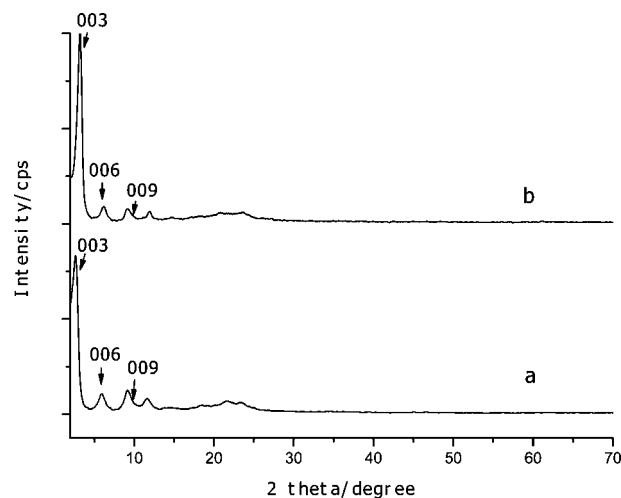


Figure 4. Powder XRD patterns of SRB-DBS/LDH thin films (a, 4.76%; and b, 9.09%).

and high crystallinity of LDH, which is favorable for the structural study of the cointercalated systems and the preparation of well-oriented films with improved polarized luminescence properties.

3.1. Characterization of the SRB-DBS/LDH Powder.

3.1.1. Crystal Structure and Composition. Figure 2A shows the XRD patterns of SRB and DBS cointercalated LDH samples SRB-DBS/LDH(x%), in which x% stands for the initial molar percentage of SRB accounting for the summation of SRB and DBS. All the patterns of these samples can be indexed to a hexagonal lattice with $R\bar{3}m$ rhombohedral symmetry. The interlayer spacing can be calculated from averaging the positions of the three harmonics: $c = 1/3 (d_{003} + 2d_{006} + 3d_{009})$. It can be

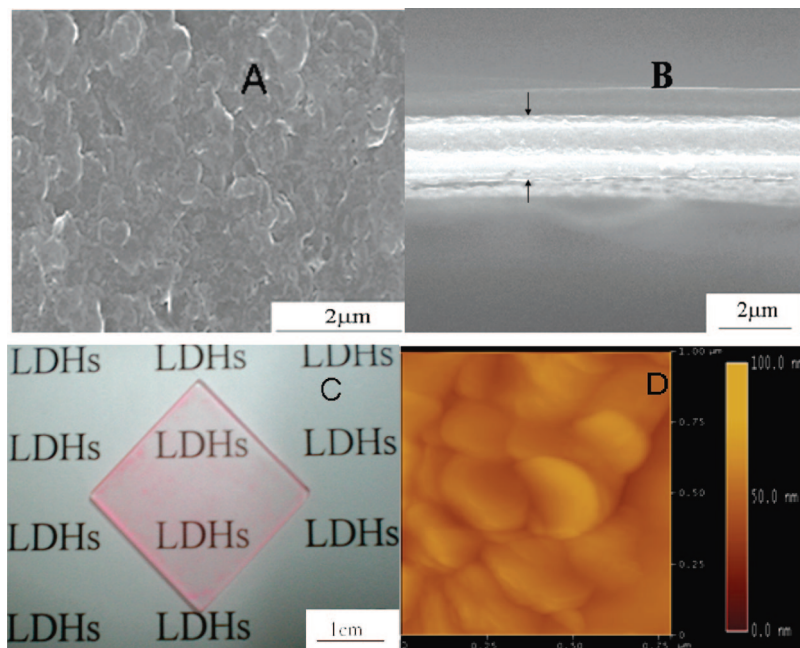


Figure 5. (A, B) The top and side views, respectively, of SEM images of SRB-DBS/LDH (9.09%) thin film. (C) The photograph of the thin film on the quartz substrate; (D) Tapping-mode AFM image of the film.

TABLE 3: Fluorescence Decay Data of the SRB-DBS/LDH (x%) Films^a

x (%)	n	τ_i (ns)	A_i (%)	$\langle \tau \rangle$ (ns)	χ^2
4.76	1	3.337	100.00	3.424	1.264
	2	3.209	96.83		
		10.000	3.17		
9.09	1	3.542	100.00	3.527	1.338
	2	3.363	76.97		
		4.076	23.03		
16.67	1	2.699	100.00	2.722	1.831
	2	3.396	53.01		
		1.961	46.99		

^a The meanings of τ_i , A_i , χ^2 , and $\langle \tau \rangle$ are the same as described in Table 2.

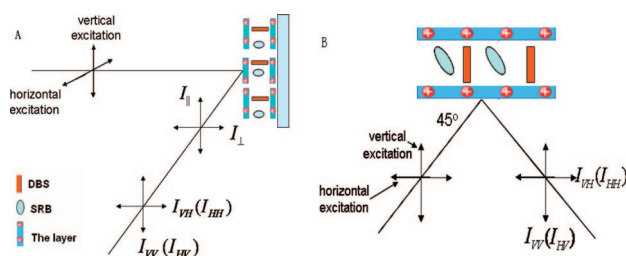


Figure 6. Schematic diagram of polarization measurement for the thin film (A and B are the measurement diagrams from different visual angles).

observed from Figure 2B that the interlayer spacing of SRB-DBS/LDH increases at first from 28.87 Å ($x = 0$) to the maximum (30.96 Å, $x = 16.67$), and then decreases gradually to the minimum (24.53 Å, $x = 100$). The variation of the interlayer spacing can be attributed to the different arrangements of interlayer guest molecules with different ratios of DBS and SRB.

The compositions of products corresponding to different initial nominal concentrations are given in Table 1. It can be seen that most of the experimental ratio of SRB to DBS in the material of SRB-DBS/LDH is close to the initial nominal ratio as expected, and it increases upon the increase of initial SRB

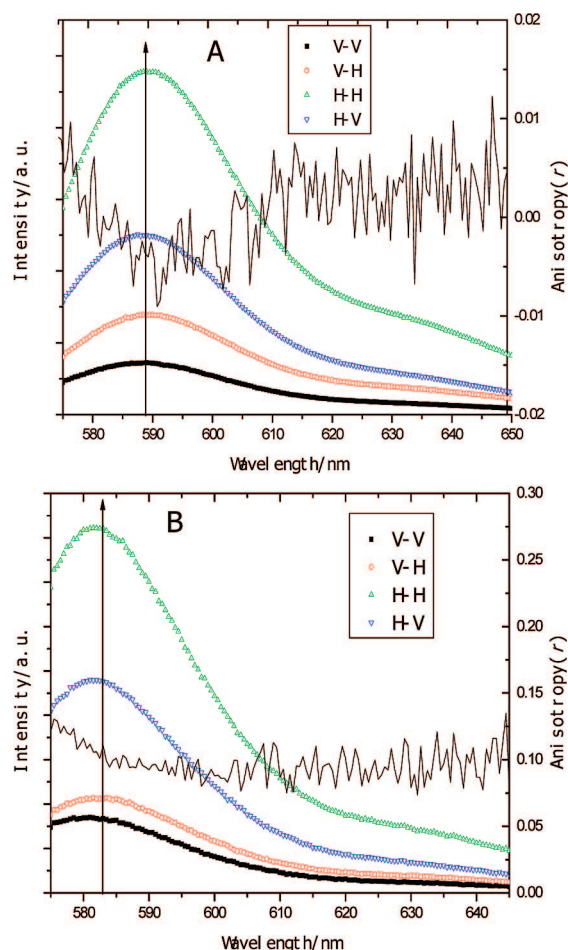


Figure 7. Photoemission profiles in the VV, VH, HH, and HV polarizations and anisotropic value (r) for the sample of SRB-DBS/LDH (9.09%) measured at room temperature (293 K): (A) powder, (B) thin film. The excitation wavelength is 570 nm.

concentration. Moreover, most of the molar ratios of Mg to Al deviate from the initial value of 2.0 and have a trend to be close

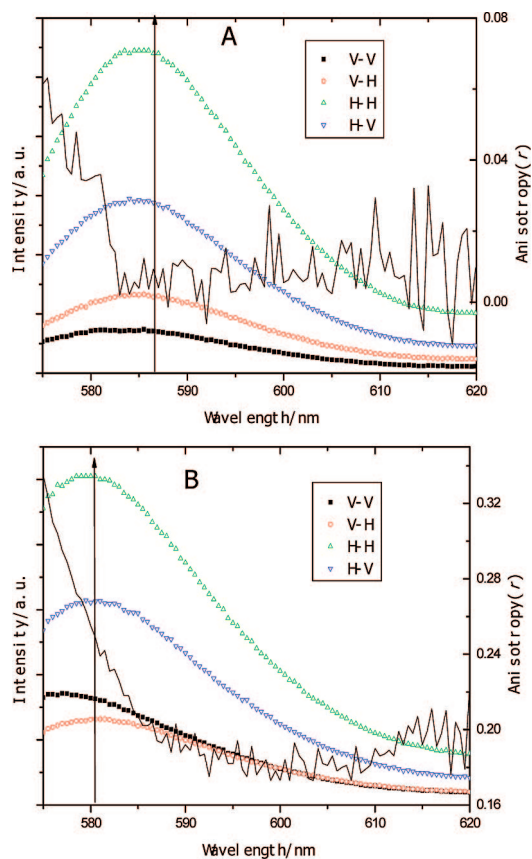


Figure 8. Photoemission profiles in the VV, VH, HH, and HV polarizations and anisotropic value (r) for the sample of SRB-DBS/LDH (9.09%) measured under the liquid nitrogen environment (77 K): (A) powder, (B) thin film. The excitation wavelength is 570 nm.

to 3.0, which may be attributed to the difference in the dissolution equilibrium between $Mg(OH)_2$ and $Al(OH)_3$ in the LDH host layer during the hydrothermal synthesis. This phenomenon has also been observed by other researchers in the study of dye intercalated LDHs.⁷

Thermolysis behavior of both pristine and intercalated SRB was studied. TG-DTA curves (see Supporting Information Figure S1) show that the sharp weight loss of SRB with three exothermic peaks appears in the range 350–500 °C, whereas the weight loss of SRB/LDH with a sharp exothermic peak occurs at ca. 600 °C, indicating that the thermal stability of SRB molecule is enhanced when intercalated into the gallery of LDHs.

3.1.2. Optimal Luminous Intensity. The fluorescence emission spectra for SRB-DBS/LDH with different molar ratios of SRB to DBS are shown in Figure 3. The fluorescence intensity increases at first to a maximum and then decreases as the ratio of SRB to DBS increases (shown in the inset plot). The optimal luminous intensity presents in the sample with 4.76% initial concentration of SRB and the emission peak appearing at 587 nm with the Full Wave at Half Maximum (FWHM) of ca. 60 nm correspond to the S_1-S_0 transition, parallel to the long axis of SRB.^{17g} The maximum emission wavelength shifts to 619 nm, and its intensity decreases quickly when the initial SRB content increases to 75%. This behavior can be attributed to the change in the state of interlayer SRB molecule. The dye exhibits a single molecular luminescence with low SRB concentrations, accounting for the increase in the luminous intensity first, and the J- or H-type dye aggregation forms when

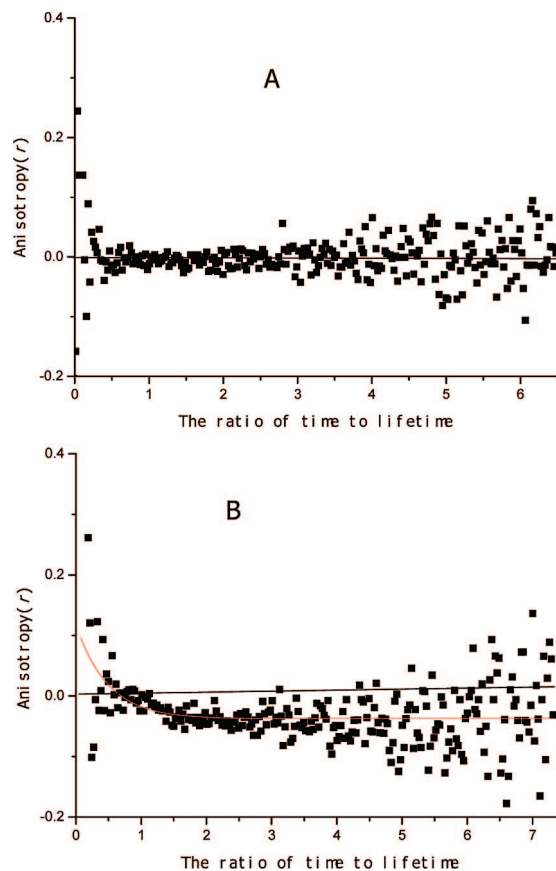


Figure 9. Time decay fluorescence anisotropy for SRB-DBS/LDH (4.76%) at room temperature (293 K): (A) powder, (B) thin film. The decay profiles were recorded with the excitation and emission wavelengths at 570 and 590 nm, respectively.

the content of SRB increases to a certain concentration, resulting in the red shift of emission spectra and the fluorescence quenching.

The solid UV–vis absorption spectra are shown in Figure 3B. The absorption intensity at 570 nm increases upon the increase of the concentration of SRB. Furthermore, another absorption shoulder band at ca. 530 nm appears when the concentration of SRB increases to 16.7%. These results confirm the aggregation of SRB in LDH when the molar percentage of SRB increases, which is both H-type (blue-shifted absorption band) and J-type (red-shifted emission band) in nature. Similar dimer aggregation was also observed in the system of Rhodamine B-doped gel glasses^{17g} and SRB adsorbed in the cationic Langmuir–Blodgett film^{17h} with high concentration of dye.

The fluorescence and absorption spectra clearly confirm that the introduction of DBS surfactant in the gallery of LDH enhances the emission intensity significantly compared with the sample of SRB intercalated LDH. Ogawa and Kuroda¹⁹ reported that surfactants or organic solvents can alter the aggregation of photoactive species. In our opinion, the intercalated long-chain surfactant molecules achieved a nonpolar interlayer environment, which homogeneously diluted and effectively isolated the interlayer SRB molecules. As a result, the distance between dye molecules is enlarged enough for preventing the formation of aggregates. In contrast, it is impossible for small inorganic anions, such as nitrate, to supply organic dye molecules with a nonpolar environment for monodispersion. Another advantage of the surfactant molecules is that they can pre-intercalate the LDH layers for enlarging the interlayer spacing, which facilitates the intercalation of bulky dye molecules. Bujdák et al.²⁰ also

TABLE 4: Fluorescence Anisotropic Value for SRB-DBS/LDH (4.76 and 9.09%) at 293 and 77 K

	293 K		77 K			
	powder	film	powder		film	
x (%)	580–620 nm	580–620 nm	580–590 nm	590–620 nm	580–590 nm	590–620 nm
4.76	0	0.10	0.02–0.08	0.02	0.15–0.22	0.15
9.09	0	0.10	0.02–0.06	0.02	0.19–0.27	0.19

TABLE 5: Orientation Correlation Time (φ), Limiting Anisotropy (r_0) and Residual Anisotropy (r_∞) for the SRB-DBS/LDH (4.76%, 9.09%) Thin Films

x (%)	orientation correlation time φ (ns)	limiting anisotropy (r_0)	residual anisotropy (r_∞)
4.76	1.674	0.118	-0.038
9.09	2.722	0.103	-0.104

found that the presence of the long-chain surfactant led to a higher emission efficiency in the system of oxazine dye intercalated cation clay, and they attributed this to the “solvating effect” of the surfactant molecules. Mohanambe et al.²¹ reported that electroneutral pyrene could also diffuse into the layers of Mg–Al–LDH after it was functionalized by anionic surfactant. It should be noted that it is important to find the optimal luminous condition for the dye and surfactant cointercalated layered matrix in actual application, not only for saving the cost of dye, but for the maximization of the luminescence efficiency.

3.1.3. Fluorescence Lifetime. The samples of SRB-DBS/LDH(x %) were studied by detecting their fluorescence decays, with excitation and emission wavelength of 570 and 587 nm, respectively. The fluorescence lifetimes were obtained by fitting

the decay profiles with one-exponential and double-exponential form respectively, and the results are tabulated in Table 2. In the double-exponential case, the average lifetime, $\langle\tau\rangle$, is also listed in Table 2.

Compared with the aqueous solution of SRB (10^{-5} mol/L, ca. 2.05 ns for one-exponential τ and 2.38 ns for $\langle\tau\rangle$) in this work, which are very close to 2.1 ns as Rifani reported²²), the fluorescence lifetime of SRB-DBS/LDH increases remarkably with x value in the range 0.99–16.7%, whereas it becomes shorter than that of the SRB solution as x increases to 25%, due to the formation of aggregation as indicated by the results of fluorescence and absorption spectra. Moreover, the longest fluorescence lifetime obtained by both one-exponential and double-exponential fitting presents for the sample of SRB-DBS/LDH (9.09%).

Ray et al.^{17h} suggested that two lifetime values can be attributed to the monomers and dimers or higher aggregates, respectively, in the study of incorporation of SRB in the octadecylamine Langmuir–Blodgett (LB) films. In this work, the very short lifetime (ca. 1–2 ns) listed in Table 2 may correspond to the aggregates of SRB in SRB-DBS/LDH, especially for the sample with high content of dye; furthermore, it was found that both τ_1 and τ_2 of SRB-DBS/LDH (4.76% and 9.09%) are much larger than those of SRB in dilute aqueous solution. The long lifetime possibly corresponds to the intercalated SRB in the gallery of LDH, and the short one is attributed to the adsorbed SRB at the surface of LDH particles, since the intercalated SRB molecule confined between the sheets is more stably immobilized. Another possible explanation for the two fluorescence lifetimes is the existence of different conformational isomers of SRB, taking into account the intercalated SRB molecules being variable depending on the LDH gallery sites.

3.2. Characterization of SRB-DBS/LDH Thin Film.
3.2.1. Orientation and Morphology. In this section, our attention was mainly focused on the two samples with SRB content of 4.76 and 9.09%, since they exhibit better photoemission behavior and longer fluorescence lifetime, respectively. As shown in Figure 4, the strong basal reflections (00 l) and the absences of any nonbasal reflections ($h, k \neq 0$) for the thin films of SRB-DBS/LDH ($x = 4.76, 9.09\%$) are as expected, taking into account the extremely well c -oriented assembly of LDH platelets.¹⁵ Moreover, this can be further confirmed by the SEM images (Figure 5, panels A and B) that the LDH lamellar crystallites are stacked with ab -plane parallel to the substrate, with the average film thickness of ca. 1.8–2 μm . As a result, it can be expected that the thin film may exhibit anisotropic light-emitting behavior. Figure 5C shows the macroscopic photograph of the transparent SRB-DBS/LDH thin film with pale pink color. The AFM topographical image (scan = 0.75 $\mu\text{m} \times 1 \mu\text{m}$) of the thin film is illustrated in Figure 5D, and the average root-mean-square (rms) roughness of the film is 12.85 nm, indicating the surface of the thin film is relative smooth.

3.2.2. Fluorescence Lifetime. The fluorescence lifetimes of SRB-DBS/LDH films ($x = 4.76, 9.09, 16.7\%$) were measured under the same conditions as powder samples mentioned above. As shown in Table 3, the SRB-DBS/LDH (9.09%) thin film

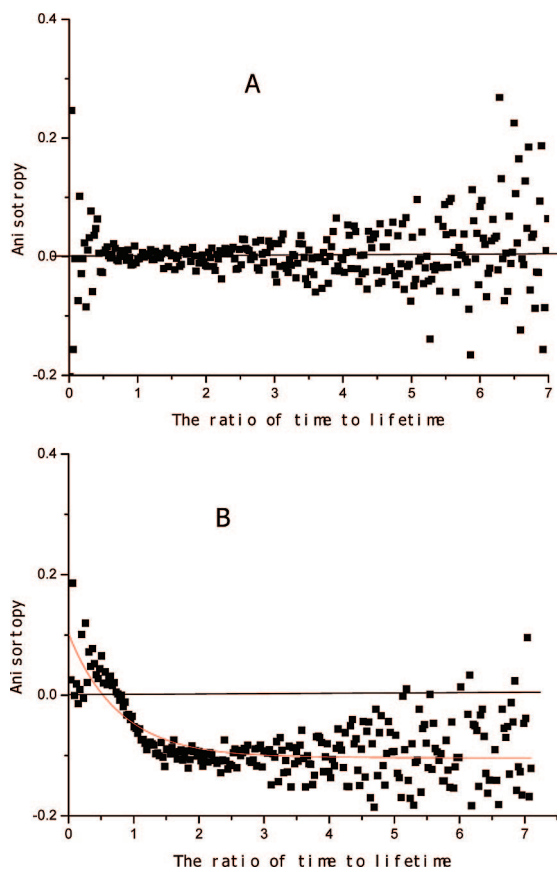


Figure 10. Time decay fluorescence anisotropy for SRB-DBS/LDH (9.09%) at room temperature (293 K): (A) powder, (B) thin film. The decay profiles were recorded with the excitation and emission wavelengths at 570 and 590 nm, respectively.

possesses the longest fluorescence lifetime and the average lifetime, which is consistent with that of the powder sample.

3.3. Comparison Studies on Polarized Fluorescence of the Powder and Film Samples. One of the most common methods to evaluate fluorescence polarization is the measurement of anisotropic value r , which was fully described by Bernard Valeur.²³ r can be expressed by the following formula,

$$r = \frac{I_{\parallel} - I_{\perp}}{I_{\parallel} + 2I_{\perp}} \text{ or } r = \frac{I_{VV} - GI_{VH}}{I_{VV} + 2GI_{VH}} \quad (1)$$

where I_{\parallel} and I_{\perp} are the photoluminescence (PL) intensity measured in the planes parallel and perpendicular to the excitation radiation, respectively. $G = (I_{HV})/(I_{HH})$; where I_{VH} is the PL intensity obtained with vertical excitation polarized and horizontal detection polarization; and I_{VV} , I_{HV} , and I_{HH} are defined in a similar way. Theoretically, the value of r is in the range from -0.2 (absorption and emission transition dipoles perpendicular) to 0.4 (two transition dipoles parallel, and deviation from this value means a reorientation of the emission dipole moment). The typical schematic diagram of fluorescence polarization measurement for the thin film is shown in Figure 6, in which the excitation and emission light keep 45° with respect to the thin film. The measurement for the powder samples is similar to that of films. It should be noted that in this measurement mode, the G factor measured based on the anisotropic film is very close to the one measured based on isotropic dye solution (see Supporting Information Figure S2).

3.3.1. Steady-State Fluorescence Polarization of the Powder and Film Samples. The polarized photoemission spectra of the SRB-DBS/LDH (4.76 and 9.09%) powder and thin film are displayed in Figure S3 (see Supporting Information) and Figure 7, respectively. It was found that the anisotropic value of the SRB-DBS/LDH (4.76 and 9.09%) powder samples is 0.0 ± 0.01 , whereas it is ca. 0.10 for the film samples, confirming that the dye-intercalated LDH thin film exhibits well-oriented and uniformly ordered behavior, as expected for the 2D structure of LDHs. However, the anisotropic value is still relatively small, which can be attributed to the rotation and translation of the SRB molecules, since the long-chain DBS supplies a flexible environment in the gallery of LDHs. As a result, the excitation and emission dipoles become somewhat deviated from each other. The evidence can be provided by the low-temperature experiment below.

It is well-known that the molecular thermal motion will be suppressed at low temperature, and thus the fluorescence depolarization of the samples may be reduced. We performed the polarization photoemission measurement for the SRB-DBS/LDH powder and film samples under the liquid nitrogen environment (77 K), and the results are shown in Figure S4 (see Supporting Information) and Figure 8, respectively. It was found that the fluorescence anisotropy of both the powder and the film samples was improved markedly, compared with that at room temperature (shown in Table 4). Moreover, slight blue shifts of photoemission peaks were observed at 77 K. The enhancement of anisotropy at low temperature results from two aspects: (1) the thermal mobility of SRB molecules was suppressed; and (2) the rigid DBS environment at 77 K restricts the rotation of SRB, which weakens the depolarization for both the powder and the film samples.

3.3.2. Time-resolved Anisotropy of the Powders and Films. Time-resolved anisotropy measurement is an important method to investigate the rotation behavior⁸ and energy transfer^{13a,b} of

luminous molecules in the time range of their fluorescence lifetime. The fluorescence anisotropy time decay profiles for SRB-DBS/LDH (4.76 and 9.09%) powder and film samples are shown in Figures 9 and 10, respectively. The anisotropy r can be expressed as:²³

$$r(t) = \frac{I_{VV}(t) - G(t)I_{VH}(t)}{I_{VV}(t) + 2G(t)I_{VH}(t)} \quad (2)$$

It is clear that the fluorescence anisotropy decay measurement of the powder samples shows no polarization, which can be assigned to the isotropic or house-of-cards structure of the LDH particles. On the contrary, the thin films exhibit an anisotropy decay effect, and the rotation behavior can be fitted by the formula as follows:²³

$$r(t) = (r_0 - r_{\infty})e^{-t/\varphi} + r_{\infty} \quad (3)$$

where r_0 is the limiting anisotropy; r_{∞} is the residual anisotropy; and φ is the orientation correlation time of the SRB molecule in the gallery of LDH. These values of different samples are tabulated in Table 5.

It is known that the orientation correlation time (φ) is the time that the anisotropy decreases to its $1/e$ of initial value. It can be found that φ of two samples are about half of corresponding fluorescence lifetime, which may suggest that the rotation of the molecule is restricted by the host layers of LDHs. Furthermore, φ of SRB-DBS/LDH (4.76%) is relatively smaller than that of SRB-DBS/LDH (9.09%), and this observation is consistent with the fact that there are more flexible DBS molecules in the gallery of LDH for SRB-DBS/LDH (4.76%), which is favorable for the transitional and rotational mobility of SRB molecule. The values of limiting anisotropy (r_0) of the two films are around 0.10 , which is in accordance with the results of steady-state polarization photoemission spectra at this wavelength. It should be noted that both the values of residual anisotropy (r_{∞}) for the two films are negative, which was seldom reported in other polarization photoemission studies.^{8,13a,b} This indicates that there is a change from $I_{\parallel} > I_{\perp}$ to $I_{\parallel} < I_{\perp}$ in the decay time range, which may arise from the rotation of SRB molecules between sheets of LDH. Since the S_1-S_0 photoemission dipole of SRB is parallel to the long axis of the chromophore,²³ the negative anisotropy may occur if the electric vector projection of emission dipole in the direction of I_{\perp} is larger than that of in the direction of I_{\parallel} (as shown in Figure S5 (see Supporting Information)). Moreover, the possibility of the energy transfer between monomer and minor aggregates in the gallery of LDH, which affects the luminescence anisotropy decay of SRB-DBS/LDH film due to the high efficiency of this energy transfer, cannot be excluded.

4. Conclusion

Photoluminescence properties of sulforhodamine B (SRB) and DBS cointercalated Mg-Al-LDH for both powder and thin film samples have been investigated. The optimal luminous intensity of SRB-DBS/LDH with 4.76% SRB molar percentage was obtained for the maximization of the luminescence efficiency. TG-DTA indicates that the thermal stability of SRB is enhanced upon intercalation. Fluorescence photoemission spectra and solid UV-vis spectra suggest the appearance of H aggregation of SRB as its content increases to 16.7%. Compared with the aqueous solution of SRB, the fluorescence lifetime of

SRB-DBS/LDH ($x\% = 0.99\text{--}16.67\%$) composites increases greatly, due to the immobilization of SRB molecule within the layered matrix. Moreover, the SRB-DBS/LDH (4.76 and 9.09%) thin films were prepared by the solvent evaporation method with well *c*-oriented morphology. The fluorescence anisotropic properties for both powder and film samples were fully investigated. Steady-state polarized luminescence measurement shows that the fluorescence anisotropic value for SRB-DBS/LDH thin film is ca. 0.10 at 293 K, which is greatly enhanced compared with that of the corresponding powder sample with no polarization. As well, the fluorescence anisotropic values of both powder and film samples were largely improved under liquid nitrogen environment. Furthermore, the SRB-DBS/LDH thin films exhibit the fluorescence anisotropy decay effect, compared with the powder sample with no anisotropy decay. The orientation correlation time (φ) of SRB-DBS/LDH (4.76%) thin film is relatively smaller than that of SRB-DBS/LDH (9.09%), which is due to the fact that there are more flexible DBS molecules in the gallery of LDHs for SRB-DBS/LDH (4.76%).

The results in this work demonstrate that the cointercalation is a reasonable and feasible method to prepare luminescent thin film materials based on LDHs, which is important for the immobilization of various luminescence and laser molecules and the functional integration of solid state photoelectronic devices. It can be expected that other functional molecules, such as electric conducting, optically active, paramagnetic ones, can also be cointercalated with dye molecules into the LDHs, from which various functional inorganic/organic hybrid devices can be designed and fabricated. Furthermore, compared with current polymer-based polarized luminescence devices obtained by liquid crystals molecules alignment,^{16a} the intrinsic structural anisotropy of LDHs resulted in the polarized luminescence of dye-intercalated LDH thin films possessing higher thermal stability. Therefore, the dye-intercalated LDH thin films should be a good candidate for solid-state polarized luminescence devices. Of course, more in-depth research should be done, which includes the increase of the fluorescence anisotropic value (r) of the SRB-DBS/LDH thin film and the molecular orientation and arrangement style of the intercalated SRB.

Acknowledgment. This work was supported by the National Natural Science Foundation of China, the Program for New Century Excellent Talents in University (Grant No.: NCET-05-121), the 111 Project (Grant No.: B07004), the Program for Changjiang Scholars and Innovative Research Team in University (Grant No.: IRT0406), and the 973 Program (Grant No.: 2009CB939802).

Supporting Information Available: TG-DTA curves of SRB and SRB intercalated LDH (Figure S1); the *G*-factor based on isotropic, anisotropic measurement modes and corresponding anisotropic values (Figure S2); polarization photoemission spectra of the SRB-DBS/LDH powders and thin films at room temperature (293K) (Figure S3); polarization photoemission spectra of the SRB-DBS/LDH powders and thin films under

the liquid nitrogen environment (77 K) (Figure S4); schematic diagram of the rotation of SRB molecule (Figure S5). This material is available free of charge via the Internet at <http://pubs.acs.org>.

References and Notes

- (1) (a) Carbonaro, C. M.; Anedda, A.; Grandi, S.; Magistris, A. *J. Phys. Chem. B* **2006**, *110*, 12932. (b) García-Moreno, I.; Costela, A.; Cuesta, A.; García, O.; del Agua, D.; Sastre, R. *J. Phys. Chem. B* **2005**, *109*, 21618.
- (2) Sels, B.; De Vos, D.; Buntinx, M.; Pierard, F.; Mesmaeker, K. D.; Jacobs, P. *Nature* **1999**, *400*, 855.
- (3) (a) Fogg, A. M.; Green, V. M.; Harvey, H. G.; O'Hare, D. *Adv. Mater.* **1999**, *11*, 1466. (b) Fogg, A. M.; Dunn, J. S.; Shyu, S. G.; Cary, D. R.; O'Hare, D. *Chem. Mater.* **1998**, *10*, 351.
- (4) (a) Yuan, Q.; Wei, M.; Evans, D. G.; Duan, X. *J. Phys. Chem. B* **2004**, *108*, 12381. (b) Choy, J.-H.; Kwak, S.-Y.; Park, J.-S.; Jeong, Y.-J.; Portier, J. *J. Am. Chem. Soc.* **1999**, *121*, 1399.
- (5) Costantino, U.; Coletti, N.; Nocchetti, M.; Aloisi, G. G.; Elisei, F. *Langmuir* **1999**, *15*, 4454.
- (6) Costantino, U.; Coletti, N.; Nocchetti, M.; Aloisi, G. G.; Elisei, F.; Latterini, L. *Langmuir* **2000**, *16*, 10351.
- (7) Bauer, J.; Behrens, P.; Speckbacher, M.; Langhals, H. *Adv. Funct. Mater.* **2003**, *13*, 241.
- (8) Mohanambe, L.; Vasudevan, S. *J. Phys. Chem. B* **2005**, *109*, 22523.
- (9) Gago, S.; Costa, T.; de Melo, J. S.; Gonçalves, I. S.; Pillinger, M. *J. Mater. Chem.* **2008**, *18*, 894.
- (10) Acharya, S.; Panda, A. B.; Efrima, S.; Golan, Y. *Adv. Mater.* **2007**, *19*, 1105.
- (11) Zhou, B.; Lin, Y.; Veca, L. M.; Fernando, K. A. S.; Harruff, B. A.; Sun, Y.-P. *J. Phys. Chem. B* **2006**, *110*, 3001.
- (12) Bovero, E.; van Veggel, F. C. J. M. *J. Phys. Chem. C* **2007**, *111*, 4529.
- (13) (a) Nguyen, T.-Q.; Wu, J. J.; Doan, V.; Schwartz, B. J.; Tolbert, S. H. *Science* **2000**, *288*, 652. (b) Nguyen, T.-Q.; Wu, J. J.; Tolbert, S. H.; Schwartz, B. J. *Adv. Mater.* **2001**, *13*, 609. (c) Wu, J. J.; Gross, A. F.; Tolbert, S. H. *J. Phys. Chem. B* **1999**, *103*, 2374. (d) Molenkamp, W. C.; Watanabe, M.; Miyata, H.; Tolbert, S. H. *J. Am. Chem. Soc.* **2004**, *126*, 4476. (e) Clark, A. P.-Z.; Shen, K.-F.; Rubin, Y. F.; Tolbert, S. H. *Nano Lett* **2005**, *5*, 1647.
- (14) (a) Okamoto, K.; Sasaki, T.; Fujita, T.; Iyi, N. *J. Mater. Chem.* **2006**, *16*, 1608. (b) Li, L.; Ma, R. Z.; Ebina, Y.; Iyi, N.; Sasaki, T. *Chem. Mater.* **2005**, *17*, 4386. (c) Liu, Z. P.; Ma, R. Z.; Osada, M.; Iyi, N.; Ebina, Y.; Takada, K.; Sasaki, T. *J. Am. Chem. Soc.* **2006**, *128*, 4872.
- (15) Gursky, J. A.; Blough, S. D.; Luna, C.; Gomez, C.; Luevano, A. N.; Gardner, E. A. *J. Am. Chem. Soc.* **2006**, *128*, 8376.
- (16) (a) Grell, M.; Bradley, D. D. C. *Adv. Mater.* **1999**, *11*, 895. (b) Chen, S. H.; Katsis, D.; Schmid, A. W.; Mastrangelo, J. C.; Tsutsui, T.; Blanton, T. N. *Nature* **1999**, *397*, 506.
- (17) (a) Arbeloa, F. L.; Chaudhuri, R.; López, T. A.; Arbeloa, I. L. *J. Colloid Interface Sci.* **2002**, *246*, 281. (b) Sasai, R.; Fujita, T.; Iyi, N.; Itoh, H.; Takagi, K. *Langmuir* **2002**, *18*, 6578. (c) Martínez, V. M.; Arbeloa, F. L.; Prieto, J. B.; López, T. A.; Arbeloa, I. L. *Langmuir* **2004**, *20*, 5709. (d) Bujdák, J.; Iyi, N. *J. Phys. Chem. B* **2005**, *109*, 4608. (e) Martínez, V. M.; Arbeloa, F. L.; Prieto, J. B.; Arbeloa, I. L. *J. Phys. Chem. B* **2005**, *109*, 7443. (f) Bujdák, J.; Martínez, V. M.; Arbeloa, F. L.; Iyi, N. *Langmuir* **2007**, *23*, 1851. (g) del Monte, F.; Levy, D. *J. Phys. Chem. B* **1998**, *102*, 8041. (h) Ray, K.; Nakahara, H. *J. Phys. Chem. B* **2002**, *106*, 92.
- (18) (a) Zhao, Y.; Li, F.; Zhang, R.; Evans, D. G.; Duan, X. *Chem. Mater.* **2002**, *14*, 4286. (b) Evans, D. G.; Duan, X. *Chem. Commun.* **2006**, 485.
- (19) Ogawa, M.; Kuroda, K. *Chem. Rev.* **1995**, *95*, 399.
- (20) Bujdák, J.; Iyi, N. *Chem. Mater.* **2006**, *18*, 2618.
- (21) Mohanambe, L.; Vasudevan, S. *J. Phys. Chem. B* **2006**, *110*, 14345.
- (22) Rifani, M.; Yin, Y.-Y.; Elliott, D. S.; Jay, M. J.; Jang, S.-H.; Kelley, M. P.; Bastin, L.; Kahr, B. *J. Am. Chem. Soc.* **1995**, *117*, 1512.
- (23) Valeur, B. *Molecular Fluorescence: Principles and Applications*; Wiley-VCH: Verlag, 2001.